ACS central science

Research Article

Cite This: ACS Cent. Sci. 2019, 5, 1170–1178

http://pubs.acs.org/journal/acscii

Neocarzilin A Is a Potent Inhibitor of Cancer Cell Motility Targeting VAT-1 Controlled Pathways

Carolin M.-L. Gleissner,[†,#] Carolin L. Pyka,[‡,#] Wolfgang Heydenreuter,[†,∥,#] Thomas F. Gronauer,[†] Carina Atzberger,[‡] Vadim S. Korotkov,[†] Weiting Cheng,[‡,⊥] Stephan M. Hacker,[§] Angelika M. Vollmar,[‡] Simone Braig,[*,‡] and Stephan A. Sieber[*,†]

[†]Center for Integrated Protein Science at the Department of Chemistry, Technische Universität München, Lichtenbergstrasse 4, Garching, D-85747, Germany

[‡]Department of Pharmacy, Pharmaceutical Biology, Ludwig-Maximilians-University of Munich (LMU), Butenandtstrasse 5-13, Munich, D-81377, Germany

[§]Department of Chemistry, Technische Universität München, Lichtenbergstrasse 4, Garching, D-85747, Germany

Supporting Information

ABSTRACT: The natural product neocarzilin A (**NCA**) was discovered decades ago, and despite its potent cytotoxic effects no mode of action studies have been performed up to date. Synthesis of neocarzilins A, B, and C and a stereoisomer of **NCA** provided insights into structural preferences as well as access to probes for functional studies. **NCA** turned out to be the most active member and was not only effective against cell proliferation but also migration, a novel and so far overlooked activity. To decipher the molecular mode of action, we applied chemical proteomics for target discovery and revealed that **NCA** targets cancer cell migration via irreversible binding to the largely uncharacterized synaptic vesicle membrane protein VAT-1. A corresponding knockout of the protein confirmed the phenotype, and pull-down studies showed the interaction with an intricate network of key migration mediators such as Talin-1. Overall, we introduce VAT-1 as a promising novel target for the development of selective migration inhibitors with the perspective to limit toxicity in the absence of antiproliferative effects.

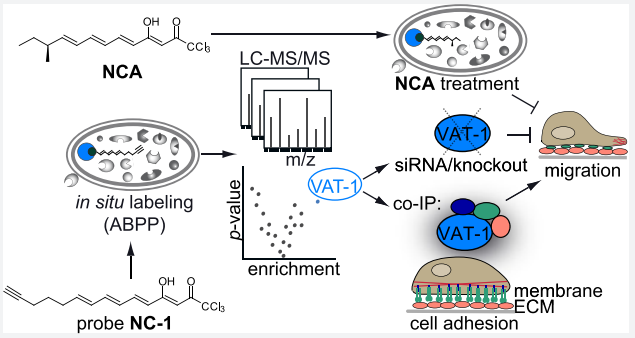

INTRODUCTION

Natural products remain a major resource for modern drug development. In cancer medicine, for example, a large fraction of all approved therapeutics is of natural origin.[1] These compounds comprise diverse structural classes such as nonribosomal peptides, alkaloids, isoprenoids, and polyketides.[2] A wealth of human targets is addressed by these molecules with hot spots in DNA-affecting proteins, cytoskeletal proteins, and tyrosine kinases. While these targets have been successfully exploited by drugs such as irinotecan and paclitaxel, as well as various kinase inhibitors, toxicity is an inevitable challenge when going after pathways essential for viability.

The exploitation of novel modes of action that do not address cell viability is, therefore, an important task requiring the discovery of suitable drug−target pairs. A closer inspection of previously identified but so far neglected structures could be a viable strategy for the identification of new anticancer leads including detailed mode of action studies. Specifically, with the advent of advanced proteomic methods for target identification such as activity-based protein profiling (ABPP), slight synthetic modifications of the parent natural product are sufficient to unravel the full complement of target proteins in living cells.[3−5] ABPP has been widely applied to unravel targets of natural products in cancer cells with a strong focus on compounds inhibiting proliferation.[6]

While inhibition of cancer cell proliferation remains a primary goal of drug development and natural product screening campaigns, inhibition of migration, the crucial step in metastasis, represents an intriguing additional pathway as the spread of cancer can be controlled and less toxicity associated side effects are to be expected.[7] Migration is a complex process initiated by actin polymerization to protrude the cell membrane and facilitate interaction with the surrounding tissue.[8] Altered integrin signaling, which is mediated by diverse integrin associated proteins such as Talin-1, fosters formation of focal adhesions to the extracellular matrix as a key step for propagating migration.[8,9] Until now, clinical development of antimigratory drugs has largely focused on a limited number of targets including integrins and matrix metalloproteinases.[10,11] To expand the spectrum of druggable targets and further

Received: March 15, 2019
Published: June 18, 2019

DOI: 10.1021/acscentsci.9b00266
ACS Cent. Sci. 2019, 5, 1170–1178

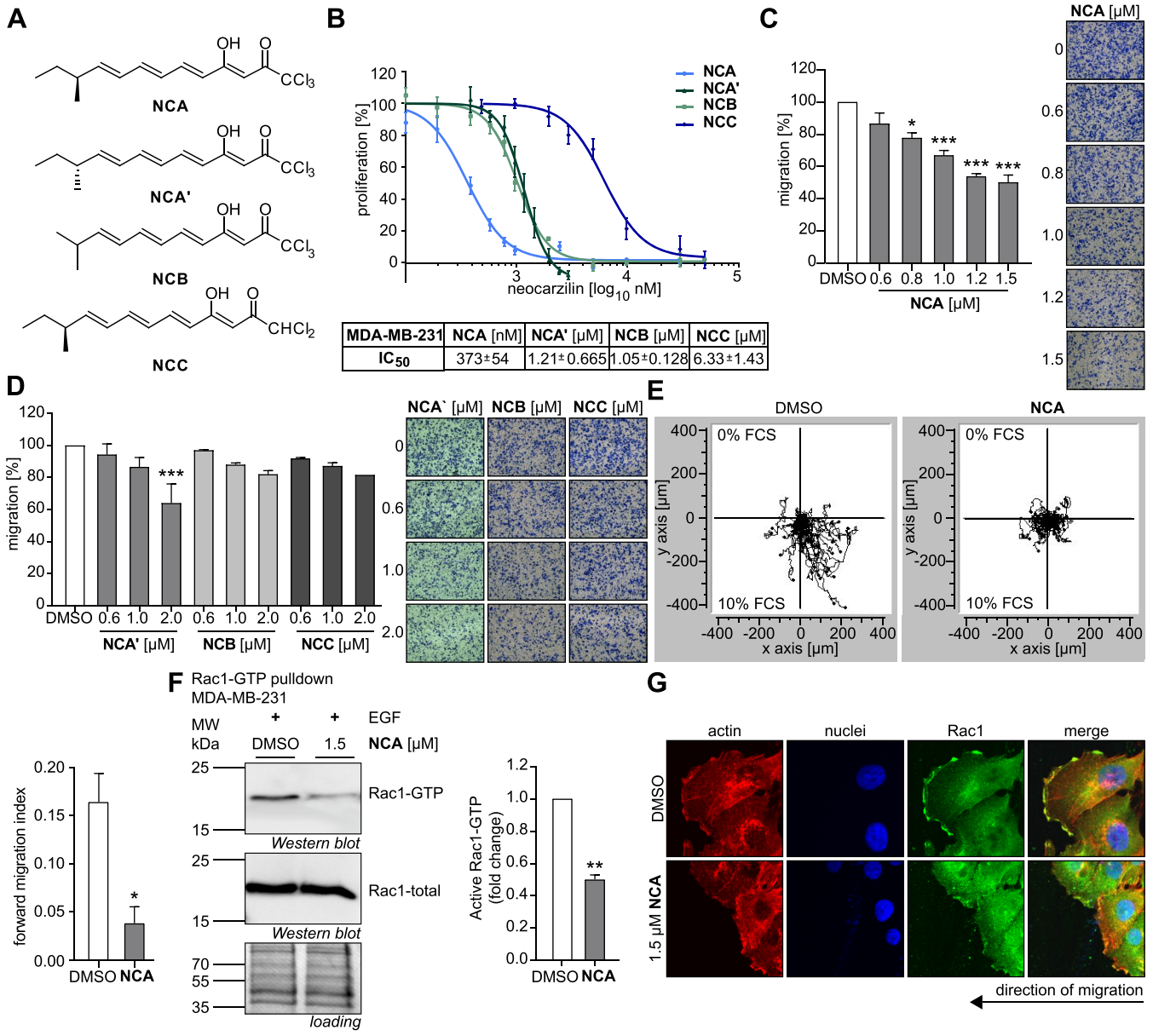

MDA-MB-231	NCA [nM]	NCA' [µM]	NCB [µM]	NCC [µM]
IC_{50}	373±54	1.21±0.665	1.05±0.128	6.33±1.43

Figure 1. Anticancer effects of neocarzilins. (A) Chemical structures of neocarzilin A, A′, B, and C. (B) Proliferative capacity of MDA-MB-231 cells treated with **NCA**, **NCA′**, **NCB**, and **NCC** and IC_{50} values determined by crystal violet staining after 72 h. (C, D) Transwell migration of MDA-MB-231 cells treated with **NCA** (C), **NCA′**, **NCB**, or **NCC** (D) determined by Boyden Chamber assay. Bar diagrams showing the number of migrated cells normalized to the control are presented; one-way ANOVA, Dunnett's test, $*P < 0.033$, $***P < 0.001$ compared with DMSO control. (B–D) Bars always represent the mean ± SEM of at least three independent experiments performed in duplicate/triplicate. (E) Trajectory blots and forward migration index as a measure of directed chemotactic migration of MDA-MB-231 cells determined by chemotaxis assay. Thirty cells per condition were monitored over 20 h. (F) Active Rac1 pull-down assay was conducted upon 5 min EGF stimulation (100 ng/mL). A representative experiment out of three independent experiments is shown. Amount of Rac1-GTP determined by Western Blot was normalized to total Rac1, and results were normalized to the control. (E, F) Bars always represent the mean ± SEM of at least three independent experiments, two-tailed unpaired Student's *t* test, $*P < 0.033$, $**P < 0.002$. (G) T24 cells treated with **NCA** were engaged in a Scratch assay and stained for Rac1 and F-actin. Nuclei were stained with Hoechst 33342. Representative images out of three independent experiments are shown.

elucidate the molecular mechanisms of migration, new chemical entities are needed. Here, natural products could serve as valuable and evolutionary preselected tools in the discovery of essential hot spots in cellular migration.[12]

In this study, the antimigratory potential of the polyenone neocarzilin A (**NCA**), produced by *Streptomyces carzinostaticus*, was investigated *in vitro* and *in vivo*. Detailed mode of action studies revealed that **NCA** irreversibly binds to VAT-1, a largely uncharacterized enzyme involved in cell migration. Accordingly, VAT-1 knockout studies matched the **NCA** phenotype of reduced motility. Whole proteome analysis paired with the identification of cellular VAT-1 interaction partners facilitated insights into an intricate regulation network highlighting that VAT-1 interacts with Talin-1, a key driver of migration.

RESULTS

Neocarzilin A Exhibits Potent Antiproliferative and Antimigratory Effects. Neocarzilins (NC) A and B, long chain polyenones bearing a characteristic trichloromethylke-

DOI: 10.1021/acscentsci.9b00266
ACS Cent. Sci. 2019, 5, 1170–1178

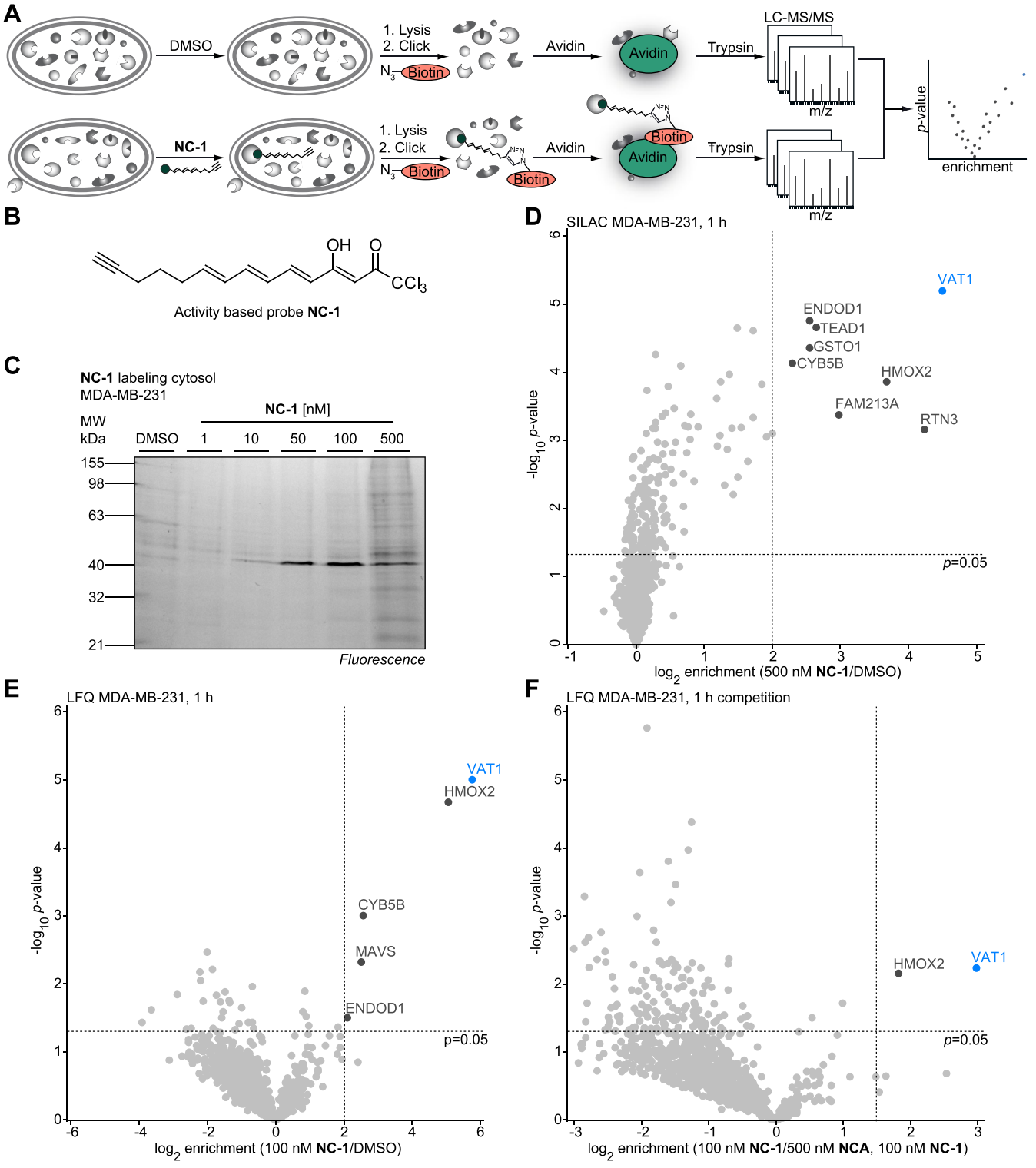

Figure 2. Identification of VAT-1 as cellular target protein of NCA by competitive LC-MS/MS-based ABPP in MDA-MB-231. (A) Schematic overview of *in situ* ABPP approach with LFQ in cancer cells with MS/MS-based read-out. (B) Chemical structure of probe **NC-1**. (C) SDS-PAGE analysis of cytosolic fraction of MDA-MB-231 after *in situ* labeling with **NC-1** for 1 h. (D) Volcano plot of *in situ* SILAC ABPP experiment with 500 nM **NC-1** ($n = 6$). Hits ($\log_2$(enrichment) > 2, p-value < 0.05) are highlighted, and the protein with the highest enrichment factor (VAT-1) is shown in blue. (E) Volcano plot of *in situ* LFQ ABPP experiment with 100 nM **NC-1** ($n = 5$). (F) Volcano plot of *in situ* competitive label-free ABPP experiment ($n = 5$) (($\log_2$(enrichment) > 1.5, p-value < 0.05). (D−F) Hits of volcano plots highlighted in dark gray are listed in Tables 4 and 5 in the SI.

tone group, were isolated in the 1990s (Figure 1A).[13] Despite their ease of synthesis and potent cytotoxicity against K562 chronic myelogenous leukemia cells with an IC_{50} of 185 nM for **NCA** (the only compound tested so far), this class of molecules attracted only little attention.[13] Studies into the corresponding polyketide biosynthesis gene cluster later

DOI: 10.1021/acscentsci.9b00266
ACS Cent. Sci. 2019, 5, 1170−1178

revealed an additional derivative termed **NCC** exhibiting a dichloro- instead of a trichloromethyl group (Figure 1A).[14] A total synthesis of **NCA** was reported and provides structural access to all members of the class for in depth functional studies.[15] Following a shortened procedure of Nozoe et al., **NCA** was synthesized in 6 steps and an overall yield of 19% (Scheme S1).[15] In brief, the synthesis of **NCA** and **NCC** started from commercially available (*S*)-2-methylbutan-1-ol, which was converted to the corresponding aldehyde via TEMPO oxidation. An *HWE* olefination, followed by a reduction/oxidation sequence yielded the *α,β,γ,δ*- unsaturated aldehyde **3**, which was transformed to trienone **4** via *Wittig* reaction. The formation of the Li-enolate and subsequent quenching with either trichloroacetic anhydride (**NCA**) or dichloroacetic anhydride (**NCC**) yielded the desired natural products. To analyze the relevance of the stereocenter, we also prepared the opposite enantiomer (**NCA′**) via an analogous reaction sequence starting from (*R*)-2-methylbutan-1-ol (Figure 1A, Scheme S2). Neocarzilin B was synthesized in a similar manner to **NCA**, starting from isobutyraldehyde (Figure 1A, Scheme S3). With all NCs in hand, we systematically analyzed their antiproliferative potency against a panel of cancer cell lines. **NCA** exhibited IC_{50} values ranging from about 300 to 800 nM for different cancer cell lines, corroborating previous literature data (Figure 1B, Figure S1A).[13] In contrast, the effects observed for **NCA′**, **NCB**, and **NCC** were less pronounced, with IC_{50} values ranging from about 1−6 μM for human MDA-MB-231 (Figure 1B) and murine 4T1-luc2 breast cancer cells (Figure S1B). Interestingly, while **NCA′**, **NCB**, and **NCC** exhibited minimal antimigratory effects in breast carcinoma cells, **NCA** significantly diminished the migration of MDA-MB-231 (Figure 1C and D). Comparable effects were obtained in 4T1-luc2 cells albeit with reduced potency of **NCA** (Figure S1C). These data suggest that already minor structural alterations in stereochemistry and the trichloromethyl group, respectively, influence the overall bioactivity. The antimigratory phenotype was also confirmed by a significant reduction of the forward migration index, a measure of directed migration, determined in a single-cell chemotaxis assay (Figure 1E). Moreover, **NCA** treatment reduced the directness of cells migrating toward a chemoattractant (Figure S1D). In addition, invasion of **NCA** treated breast cancer cells was also severely impaired (Figure S1E). **NCA** had no apoptotic effects on MDA-MB-231 cells at concentrations which are relevant for inhibition of migration (Figure S1F). Of note, apoptosis assays of **NCA** treated 4T1-luc2 cells revealed minor induction of cell death at concentrations and time points considerable for migration inhibition (Figure S1G), which could slightly impact the antimigratory readout. Whereas cell cycle progression and microtubule network organization were not affected by **NCA** (Figure S1H and I), activation of the small Rho GTPase Rac1 was compromised in **NCA** treated cells as shown by Rac1 pulldown assays (Figure 1F). In addition, confocal microscopy images demonstrated reduced formation of lamellipodia and aberrant localization of Rac1 in migrating cancer cells treated with **NCA** (Figure 1G). In order to investigate the *in vivo* efficacy of **NCA**, luciferase tagged 4T1 murine cells were injected into the tail vein of Balb/c mice.[16] Treatment with 10 mg/kg of **NCA** was suggested to reduce tumor cell dissemination into the mouse lungs compared to solvent control treated animals after 5 days (Figure S1J). Of note, the body weight of the mice during the experiment increased in both groups, thus suggesting a suitable safety profile of the compound (Figure S1J).

Chemical Proteomics Identify VAT-1 As Cellular Target of Neocarzilin A. To unravel **NCA**'s mode of action, we applied ABPP for target discovery and designed a corresponding alkynylated probe **NC-1** (Figure 2A and B, Scheme 1). Given the importance of the trichloromethyl group

Scheme 1. Synthesis of Probe NC-1: (a) 1. DMSO (2.22 equiv), $(COCl)_2$ (1.11 equiv), NEt_3 (4.50 equiv); 2. LiHMDS (1.00 equiv), Ethyl (E)-4-(Diethoxyphosphoryl)-but-2-enoate (4.15) (1.00 equiv), CH_2Cl_2, THF, −78 °C → rt, 4 h, 38% over Two Steps; (b) DIBAL-H (2.10 equiv), MnO_2 (20.0 equiv), THF, Hexane, −78 °C → rt, 5 h, 54% over Two Steps; (c) 1-(Triphenyl-phosphoranylidene)-2-propanone (2.00 equiv), Toluene, 100 °C, 16 h, 54%; (d) 1. LiHMDS (2.00 equiv); 2. Trichloroacetic Anhydride (1.00 equiv), THF, −78 °C, 3 h, 45%

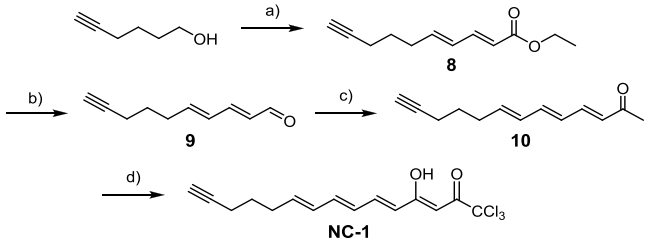

for biological activity, we hypothesized that this electrophilic structural element might covalently interact with the dedicated protein target. Thus, probe design commenced with an **NCA** analog bearing a terminal alkyne at the polyene tail (Scheme 1). Upon *in situ* protein binding and subsequent cell lysis, the alkyne serves as a unique handle to identify protein targets via click chemistry (CC) to biotin azide, avidin enrichment, and quantitative LC-MS/MS analysis (Figure 2A).[17−20] The synthetic strategy followed the established natural product assembly and utilized hexyn-1-ol as a starting material (Scheme 1). The resulting Neocarzilin probe (**NC-1**) was tested for antiproliferative and antimigratory effects. As depicted in Figure S2A, the antiproliferative activity significantly dropped in MDA-MB-231 and 4T1-luc2 cells (IC_{50}'s of 24−34 μM) compared to **NCA**. In contrast the antimigratory activity was only slightly reduced (Figure S2B). In accordance with the results obtained with **NCA**, neither cell death nor induction of apoptosis was observed upon treatment of the breast carcinoma cell lines with **NC-1** (Figure S2C and D). Overall, these results suggest that the probe is suitable for the labeling of NC antimigratory targets. Prior to MS studies, optimal labeling conditions were adjusted via gel-based analysis of probe treated MDA-MB-231, MCF-7, HepG2, and T24 cells followed by CC to rhodamine azide and subsequent fluorescent SDS-PAGE (Figures 2C, S3A and B). One intense 40 kDa protein band was observed in all four cell lines after 1 h of probe incubation. This band remained visible even at low concentrations of 10−100 nM and was outcompeted by the addition of 1- and 5-fold **NCA** (Figure S3C). The labeling of this band remained even after extended incubation times of 24 and 48 h suggesting sufficient stability upon binding of the protein target (Figure S3D). To unravel the identity of all targets in MDA-MB-231 and HepG2 cells, two complementary proteomic procedures, *i.e.*, stable isotope labeling of amino acids in cell culture (SILAC) and label-free quantification

DOI: 10.1021/acscentsci.9b00266
ACS Cent. Sci. 2019, 5, 1170−1178

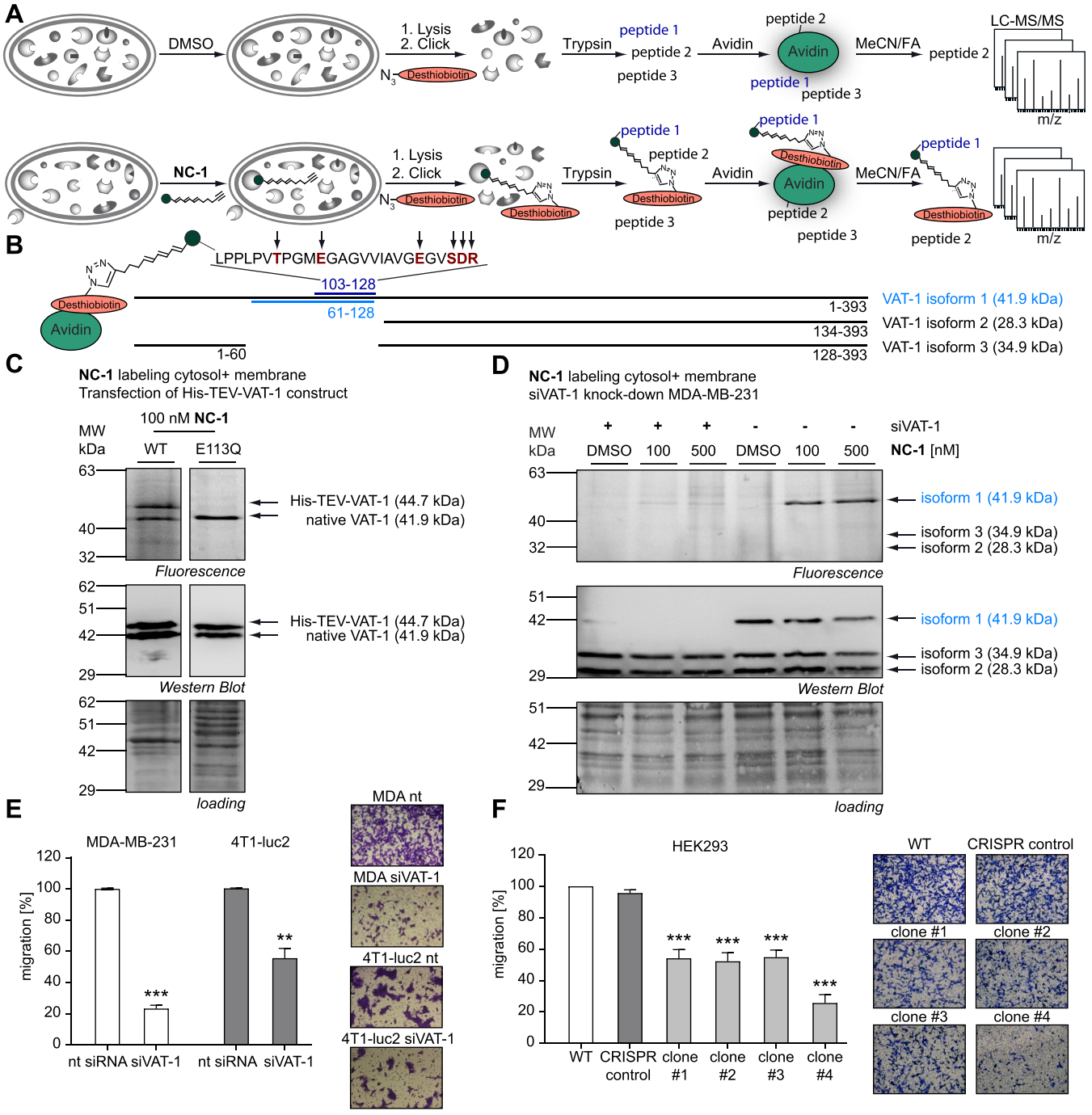

Figure 3. Verification of VAT-1 as a target protein and its effect on cell migration. (A) Schematic overview of ABPP based approach to identify binding site peptides. After protein digestion, only peptides bound to the probe are enriched on avidin beads and eluted with acetonitrile (MeCN) and formic acid (FA) for MS/MS detection. (B) Identified binding site peptide (aa 103−128) in **NC-1** treated cells and location of the peptide in the part of VAT-1, which is unique to isoform 1. Mutated residues are shown in red. (C) *In situ* labeling of MDA-MB-231, which were transfected with His-TEV-VAT-1 construct expressing wildtype (WT) or the point mutant E113Q. (D) Analytical labeling of siVAT-1 knockdown cells in comparison to control-treated cells. (E, F) Transwell migration of (nontargeting) nt and VAT-1 siRNA transfected MDA-MB-231 and 4T1-luc2 cells (E) and of HEK293 CRISPR-Cas9 VAT-1 knockout clones (F) determined by Boyden Chamber assay. Bar diagrams show the number of migrated siVAT-1 cells normalized to nt siRNA cells (E) or VAT-1 knockout cells (F) normalized to WT cells. Unsuccessfully altered WT cells were included as an additional control (*CRISPR control*) in F. (E,F) Bars represent the mean ± SEM of at least three independent experiments performed in duplicate, two-tailed unpaired Student's *t* test, $^{**}P < 0.002$, $^{***}P < 0.001$ (E), one-way ANOVA, Dunnett's test, $^{***}P < 0.001$ compared with DMSO control (F).

(LFQ), were applied to maximize the overall confidence of obtained hits.[21,22] Cells were incubated with 100−500 nM **NC-1** or DMSO as a background control and processed for LC-MS/MS proteome analysis (Figures 2D and E, S4A and B). Detected proteins are visualized in volcano plots displaying enrichment over the background ($\log_2$(enrichment) > 2) on the *x*-axis and significance ($p < 0.05$) on the *y*-axis. Importantly, both SILAC and LFQ revealed comparable

DOI: 10.1021/acscentsci.9b00266
ACS Cent. Sci. 2019, 5, 1170−1178

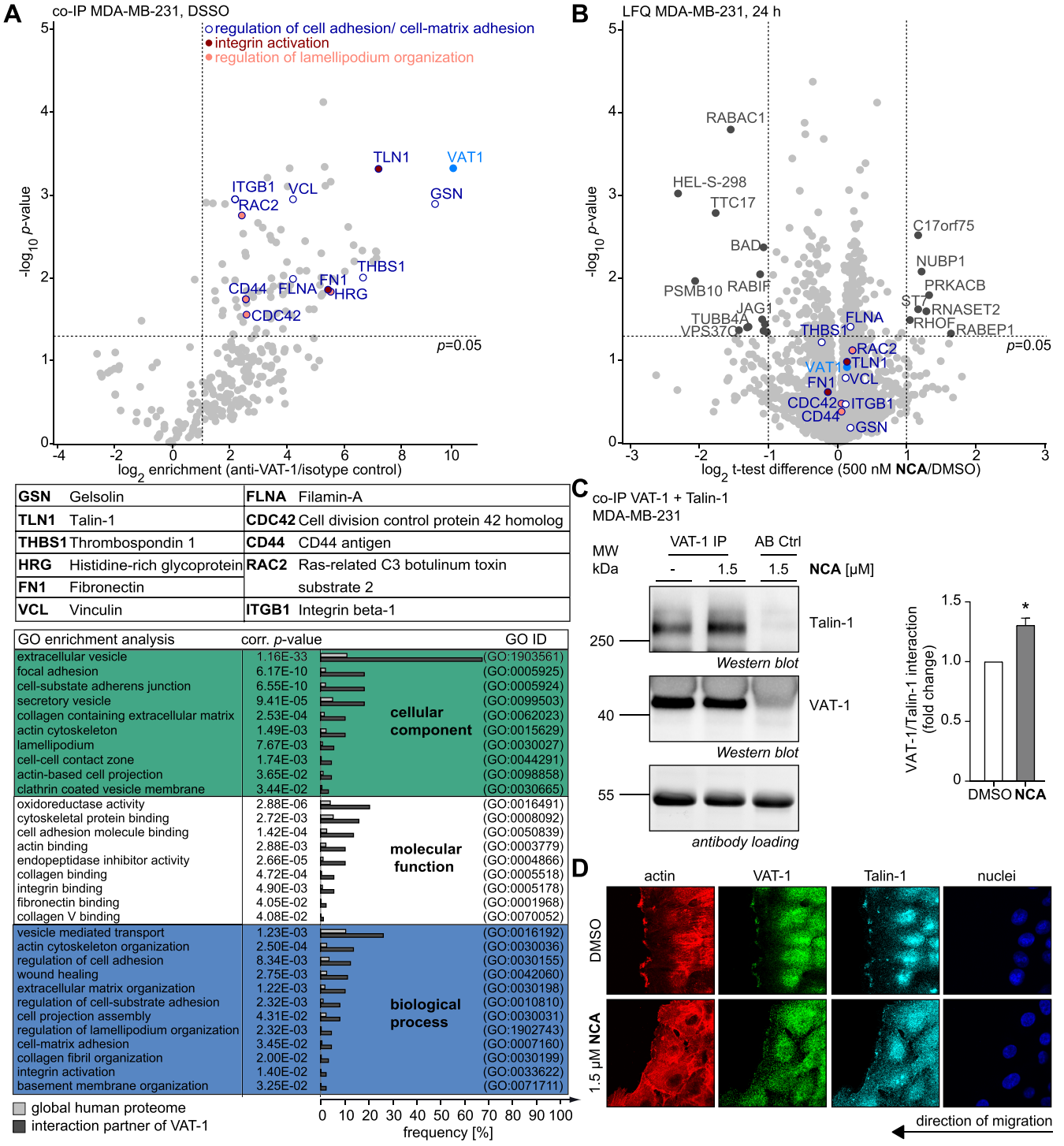

Figure 4. Cellular pathways and interaction partner of VAT-1 in the context of cell migration. (A) Volcano plot of co-IP of VAT-1 with 2 mM DSSO in MDA-MB-231 (n = 3). GO enrichment analysis of hits (($\log_2$(enrichment) > 1, p-value < 0.05) was performed with the Cytoscape[29] BINGO app[30] (SI Tables 8−10), whereas frequencies of enriched GO terms are compared between the co-IP and the global proteome. (B) Volcano plot of global proteome analysis with LFQ in MDA-MB-231 treated with 500 nM **NCA** for 24 h (n = 6). Proteins identified in the co-IP in A are shown with the same color code. (A,B) Hits of volcano plots are listed in Tables 6 and 7 in the SI. (C) Co-IP of VAT-1 and Talin-1. VAT-1 was precipitated from MDA-MB-231 cell lysates after 24 h of stimulation with **NCA**. Amount of Talin-1 determined by Western blot was normalized to VAT-1, and results were normalized to the control. Bars represent the mean ± SEM of two independent experiments, two-tailed unpaired Student's t test, *P < 0.033. (D) T24 cells treated with **NCA** were engaged in a Scratch assay and costained for VAT-1 (green), Talin-1 (cyan), and actin (red). Nuclei were stained with Hoechst 33342. (C,D) A representative experiment out of three independent experiments is shown.

results with one protein protruding as the most significant and highly enriched target in both cell lines, namely, the synaptic vesicle membrane protein (VAT-1, 41.2 kDa; Figures 2D and E, S4A and B). This direct comparison of SILAC and LFQ analysis in ABPP studies demonstrates the adequate and reproducible readout of both methods. To further enhance the

DOI: 10.1021/acscentsci.9b00266
ACS Cent. Sci. 2019, 5, 1170−1178

confidence of the identified targets, competitive studies with an excess of 5-fold **NCA** were performed via LFQ in both cell lines (Figures 2F, S4C). Again, extended incubation times with 500 nM **NC-1** for 24 h did not change the result (Figure S4D). Overall, VAT-1 was presented by far as the best hit in enrichment as well as competition experiments throughout both cell lines. Most of the hits either represent additional proteins of high abundance frequently targeted by electrophilic compounds (e.g., heme oxygenase HMOX2) or displayed insufficient competition (Figures 2F, S4C). These proteins were thus discarded from further analysis and VAT-1 selected for validation.

VAT-1 Plays an Essential Role in Cancer Cell Migration. To confirm VAT-1 as a target of **NCA** directly, we prepared the recombinant protein *via* overexpression in *E. coli*. Gel-based labeling with **NC-1** and fluorescent tagging revealed a clear protein band for *E. coli* lysate after overexpression as well as the recombinant protein (Figure S5A and B). Heat inactivation of the protein prior to labeling strongly reduced the signal, demonstrating binding of the probe and the natural product to the folded and active protein (Figure S5B). Despite intense efforts including MS/MS fragmentation of the labeled protein (purified and endogenous) as well as by applying a strategy to detect the modified peptide using a cleavable linker or a desthiobiotin modification (Figure 3A), we were unable to decipher the **NCA** binding site. However, we detected an unmodified tryptic peptide by MS/MS, which was eluted from the beads after desthiobiotin enrichment, suggesting that the probe was detached during the MS preparation procedure. In order to confirm this peptide and further narrow down the binding site, we sequentially mutated all nucleophilic amino acids within its sequence (Figure 3B). The resulting His-TEV-VAT-1 constructs were tested for probe labeling in MDA-MB-231, and solely in case of the E113Q mutant, no fluorescent gel band could be observed (Figures 3C, S5C). Of note, the corresponding peptide is only present in one out of three native VAT-1 isoforms (Figure 3B), which are all expressed in MDA-MB-231. Solely the E113 containing isoform is labeled by the probe further corroborating the correct localization of the **NCA** binding site (Figure 3D). Several additional targets of **NCA** represent proteins with highly electrophile-sensitive cysteine residues (e.g., GSTO1 (C32), HMOX2 (C265, C282), FAM213A (C85,C88)), which suggests that the trichloromethyl ketone group of **NCA** has some potential for reacting with cysteine residues as well.[23−25]

Previous studies showed increased mRNA and protein levels of VAT-1 in glioblastomas and benign prostatic hyperplasia compared to healthy tissue.[26,27] A corresponding siRNA based VAT-1 knockdown significantly impaired glioma cell migration but not proliferation.[26] This functional link to cancer cell motility matches the observed phenotype of **NCA** and merits further investigation. MDA-MB-231 cells transfected with siRNA against VAT-1 displayed significantly reduced labeling of the signature 40 kDa protein with **NC-1**, thus directly confirming its identity as VAT-1 and independently validating the MS results (Figure 3D, successful knockdown of VAT-1 in siRNA transfected cells is shown in Figure S6A).

VAT-1 knockdown in MDA-MB-231 and 4T1-luc2 cells had no effect on apoptosis (Figure S6B) and caused 50−80% inhibition of migration (Figures 3E, S6C). At the same time, proliferation was unaffected (Figure S6D). In addition, CRISPR-Cas9 VAT-1 knockout clones were generated by deleting exon 2 of VAT-1 in HEK293 cells (Figure S6E). In comparison to wildtype HEK293 cells and mock-transfected cells (CRISPR control), the VAT-1 knockout clones displayed a strong impairment of migration (to a comparable extent to that observed with **NCA**; Figure 3F), whereas the proliferative capacity of these cells was not altered (Figure S6F). While this supports that **NCA**'s cell motility phenotype is predominantly mediated through VAT-1 inhibition, it suggests that the antiproliferative effect could be contributed via a different target.

VAT-1/Talin-1 Interaction. Given the strong impact of **NCA** on migration, we further focused on elucidating the functional role of VAT-1 in cancer metastasis via proteomic studies. Co-immunoprecipitation (co-IP) with an immobilized anti-VAT-1 antibody was carried out in the presence of the DSSO cross-linker in order to capture also transient interactions as shown previously.[28] Subsequent analysis of pulled down proteins via LC-MS/MS revealed several significantly enriched hits in MDA-MB-231 cells (Figure 4A). In comparison, the overall effect of **NCA** on the total proteome was very limited, and no significant effect of **NCA** on the expression of co-IP hits could be observed, which was further corroborated by independent Western blot data (Figure 4B, Figure S7). Interestingly, several of the identified VAT-1 interaction partners functionally cluster into the regulation of cell adhesion (e.g., gelsolin, GSN; fibronectin, FN1), integrin activation (e.g., Talin-1, TLN), and lamellipodium organization (e.g., RAC2). Foremost, Talin-1, an important activator of integrins and thus involved in regulating migration, protruded as one of the strongest hits. The interaction with Talin-1 could be independently verified by a Western blot-based co-IP assay, in which VAT-1 was pulled down from whole cell lysates (Figure 4C). Of note, treatment of the cells with **NCA** seemed to even further enhance the interaction of VAT-1 with Talin-1 (Figure 4C). Moreover, immunostaining revealed colocalization of both proteins in lamellipodia at the leading edge of migrating cells (Figure 4D).

DISCUSSION

The detailed investigation of **NCA** in the context of cancer decades after its discovery demonstrates the power of chemical proteomics. While the molecule was only known for potent cell toxicity,[13] its antimigratory effects have been overlooked. By investigating the impact of **NCA** and its derivatives on the inhibition of migration and elucidating its mode of action *via* ABPP-based target-fishing approaches, we demonstrate that VAT-1 is a promising novel drug target in cancer research. This largely uncharacterized protein emerges as the by far most prominent hit in both SILAC and LFQ methodologies as well as in competitive labeling approaches, which emphasizes the high specificity of **NCA** to its target VAT-1. Interestingly, no other proteins presented as prominent hits, suggesting that our simplified probe design lacking the methyl-stereocenter of **NCA** may have lost affinity for the target(s) responsible for the antiproliferative effects. The importance of this stereocenter was corroborated by synthesis of **NCA**′ bearing the opposite absolute configuration, resulting in a drop in potency.

Although we were unable to decipher the exact binding mode of **NCA** to VAT-1, we identified the region of the protein that is modified and unraveled E113 as the likely point of irreversible attachment. Future studies involving cocrystallization will have to show how this interaction affects the function of the protein on a molecular level.

DOI: 10.1021/acscentsci.9b00266
ACS Cent. Sci. 2019, 5, 1170−1178

Little is known to date about VAT-1: It is proposed to play a role in cancer cell motility and shows putative ATPase activity and calcium dependency.[26,31,32] In addition, a homology to *E. coli* quinone oxidoreductases as well as eye lens zeta-Crystallin has been described.[33] The present study further illustrates that inhibiting the expression of VAT-1 either by specific siRNA or CRISPR-Cas9 knockout strongly abrogates migration of the cells, thus paralleling the robust biological antimigratory effects of **NCA**. Of note, in contrast to the effect of **NCA** on inhibition of proliferation, genetically impairing VAT-1 expression does not affect cellular growth. Hence, whereas the antimigratory effects of **NCA** are mediated by its target VAT-1, further studies will focus on the so far unknown binding partners of **NCA**, which are implicated in inhibition of proliferation.

Proteome analysis to unravel the role of VAT-1 in regulating cellular migration revealed that VAT-1 interacts with a network of proteins associated with cell motility. Intriguingly, Talin-1 could be identified as a direct interaction partner of VAT-1 both by MS-based co-IP experiments as well as by immunoblotting. Talin-1 is one of the key proteins activating integrin signaling, mediating linkage of integrins to the cytoskeleton, formation of focal adhesions, and subsequently promoting migration.[34] Although treatment of the cells with **NCA** seemed to enhance the interaction of its target VAT-1 with Talin-1, future studies need to elucidate how this interaction regulates this network on a molecular level.

In summary, VAT-1 could be identified as a so far unknown player in regulation of cancer cell migration that directly interacts with crucial cell migration proteins such as Talin-1. Moreover, with the identification of **NCA** as a potent migration inhibitor, chemically easily assessable VAT-1 probes are now available for further studies. Hence, VAT-1 with its unique mode of action is set on stage as a novel drug target for anticancer strategies preventing migration and metastasis.

■ ASSOCIATED CONTENT

Supporting Information

The Supporting Information is available free of charge on the ACS Publications website at DOI: 10.1021/acscentsci.9b00266.

Additional text, figures, tables and schemes giving biochemical data, labeling results, synthetic strategies, compound characterization data, and ^{1}H and ^{13}C NMR spectra (PDF)

■ AUTHOR INFORMATION

Corresponding Authors

*E-mail: simone.braig@cup.uni-muenchen.de.
*E-mail: stephan.sieber@tum.de.

ORCID

Stephan M. Hacker: 0000-0001-5420-4824
Stephan A. Sieber: 0000-0002-9400-906X

Present Addresses

[‖]Department for Organic Chemistry, ETH Zurich, Vladimir-Prelog-Weg 1-5/10, 8093 Zürich, Switzerland
[⊥]Department of Oncology, Wuhan No. 1 Hospital, Zhongshan Ave. 215, 430022, Hubei, China

Author Contributions

[#]C.M.-L.G., C.L.P., and W.H. contributed equally to this work.

Funding

We gratefully acknowledge funding from the Deutsche Forschungsgemeinschaft (DFG) SI 1096/12-1, FOR1406, and the Center for Integrated Protein Science Munich (CIPSM). S.M.H. acknowledges financial support from a Liebig fellowship of the Fonds der Chemischen Industrie.

Notes

The authors declare no competing financial interest.

■ ACKNOWLEDGMENTS

We thank Stefan Zahler for review of microscopy data and Julie Petry for help in experiments conducted with CRISPR knockout cells as well as Julia Blenninger and Kerstin Loske for general technical support. Furthermore, we would like to acknowledge Mona Wolff, Katja Bäuml, and Katja Gliesche for technical assistance as well as interns Lisa Schweizer, Lena Kastner, Ramona Absmeier, Imke Lemmer, Anton Murnauer, and Patrick Zanon for helping with experiments. Further, we thank the Department of Oncology of the Wuhan No. 1 hospital in Hubai for the support.

■ ABBREVIATIONS

VAT-1, synaptic vesicle membrane protein VAT-1; ABPP, activity-based protein profiling; NC, Neocarzilin; CC, click chemistry; SILAC, stable isotope labeling of amino acids in cell culture; LFQ, label-free quantification; WT, wildtype; CRISPR, clustered regularly interspaced short palindromic repeats; co-IP, coimmunoprecipitation; FN1, Fibronectin; GSN, Gelsolin; TLN1, Talin-1; Rac2, Ras-related C3 botulinum toxin substrate 2; siRNA, small interfering RNA

■ REFERENCES

(1) Newman, D. J.; Cragg, G. M. Natural products as sources of new drugs from 1981 to 2014. *J. Nat. Prod.* **2016**, *79* (3), 629−661.
(2) Santos, R.; Ursu, O.; Gaulton, A.; Bento, A. P.; Donadi, R. S.; Bologa, C. G.; Karlsson, A.; Al-Lazikani, B.; Hersey, A.; Oprea, T. I.; Overington, J. P. A comprehensive map of molecular drug targets. *Nat. Rev. Drug Discov.* **2017**, *16* (1), 19−34.
(3) Evans, M. J.; Cravatt, B. F. Mechanism-based profiling of enzyme families. *Chem. Rev.* **2006**, *106* (8), 3279−3301.
(4) Gersch, M.; Kreuzer, J.; Sieber, S. A. Electrophilic natural products and their biological targets. *Nat. Prod. Rep.* **2012**, *29* (6), 659−682.
(5) Fonovic, M.; Bogyo, M. Activity-based probes as a tool for functional proteomic analysis of proteases. *Expert Rev. Proteomics* **2008**, *5* (5), 721−730.
(6) Liu, Y.; Guo, M. Chemical proteomic strategies for the discovery and development of anticancer drugs. *Proteomics* **2014**, *14* (4−5), 399−411.
(7) Mackay, C. R. Moving targets: cell migration inhibitors as new anti-inflammatory therapies. *Nat. Immunol.* **2008**, *9* (9), 988−998.
(8) Friedl, P.; Wolf, K. Tumour-cell invasion and migration: diversity and escape mechanisms. *Nat. Rev. Cancer* **2003**, *3* (5), 362−374.
(9) Lagarrigue, F.; Vikas Anekal, P.; Lee, H. S.; Bachir, A. I.; Ablack, J. N.; Horwitz, A. F.; Ginsberg, M. H. A RIAM/lamellipodin-talin-integrin complex forms the tip of sticky fingers that guide cell migration. *Nat. Commun.* **2015**, *6*, 8492.
(10) Raab-Westphal, S.; Marshall, J. F.; Goodman, S. L. Integrins as therapeutic targets: successes and cancers. *Cancers (Basel)* **2017**, *9* (9), 110.
(11) Radisky, E. S.; Raeeszadeh-Sarmazdeh, M.; Radisky, D. C. Therapeutic potential of matrix metalloproteinase inhibition in breast cancer. *J. Cell. Biochem.* **2017**, *118* (11), 3531−3548.

DOI: 10.1021/acscentsci.9b00266
ACS Cent. Sci. 2019, 5, 1170−1178

(12) Sarwar, M. S.; Zhang, H. J.; Tsang, S. W. Perspectives of plant natural products in inhibition of cancer invasion and metastasis by regulating multiple signaling pathways. *Curr. Med. Chem.* **2018**, *25* (38), 5057−5087.
(13) Nozoe, S.; Ishii, N.; Kusano, G.; Kikuchi, K.; Ohta, T. Neocarzilins A and B, novel polyenones from Streptomyces carzinostaticus. *Tetrahedron Lett.* **1992**, *33*, 7547−7550.
(14) Otsuka, M.; Ichinose, K.; Fujii, I.; Ebizuka, Y. Cloning, sequencing, and functional analysis of an iterative type I polyketide synthase gene cluster for biosynthesis of the antitumor chlorinated polyenone neocarzilin in "Streptomyces carzinostaticus". *Antimicrob. Agents Chemother.* **2004**, *48* (9), 3468−3476.
(15) Nozoe, S.; Kikuchi, K.; Ishii, N.; Ohta, T. Synthesis of neocarzilin A: An absolute stereochemistry. *Tetrahedron Lett.* **1992**, *33*, 7551−7552.
(16) Braig, S.; Kressirer, C. A.; Liebl, J.; Bischoff, F.; Zahler, S.; Meijer, L.; Vollmar, A. M. Indirubin derivative 6BIO suppresses metastasis. *Cancer Res.* **2013**, *73* (19), 6004−6012.
(17) Rostovtsev, V. V.; Green, L. G.; Fokin, V. V.; Sharpless, K. B. A stepwise huisgen cycloaddition process: copper(I)-catalyzed regioselective "ligation" of azides and terminal alkynes. *Angew. Chem. Int. Ed. Engl.* **2002**, *41* (14), 2596−2599.
(18) Tornoe, C. W.; Christensen, C.; Meldal, M. Peptidotriazoles on solid phase: [1,2,3]-triazoles by regiospecific copper(i)-catalyzed 1,3-dipolar cycloadditions of terminal alkynes to azides. *J. Org. Chem.* **2002**, *67* (9), 3057−3064.
(19) Wright, M. H.; Tao, Y.; Drechsel, J.; Krysiak, J.; Chamni, S.; Weigert-Munoz, A.; Harvey, N. L.; Romo, D.; Sieber, S. A. Quantitative chemoproteomic profiling reveals multiple target interactions of spongiolactone derivatives in leukemia cells. *Chem. Commun. (Cambridge, U. K.)* **2017**, *53* (95), 12818−12821.
(20) Speers, A. E.; Adam, G. C.; Cravatt, B. F. Activity-based protein profiling in vivo using a copper(i)-catalyzed azide-alkyne [3 + 2] cycloaddition. *J. Am. Chem. Soc.* **2003**, *125* (16), 4686−4687.
(21) Ong, S. E.; Blagoev, B.; Kratchmarova, I.; Kristensen, D. B.; Steen, H.; Pandey, A.; Mann, M. Stable isotope labeling by amino acids in cell culture, SILAC, as a simple and accurate approach to expression proteomics. *Mol. Cell. Proteomics* **2002**, *1* (5), 376−386.
(22) Cox, J.; Hein, M. Y.; Luber, C. A.; Paron, I.; Nagaraj, N.; Mann, M. Accurate proteome-wide label-free quantification by delayed normalization and maximal peptide ratio extraction, termed MaxLFQ. *Mol. Cell. Proteomics* **2014**, *13* (9), 2513−2526.
(23) Backus, K. M.; Correia, B. E.; Lum, K. M.; Forli, S.; Horning, B. D.; Gonzalez-Paez, G. E.; Chatterjee, S.; Lanning, B. R.; Teijaro, J. R.; Olson, A. J.; Wolan, D. W.; Cravatt, B. F. Proteome-wide covalent ligand discovery in native biological systems. *Nature* **2016**, *534* (7608), 570−574.
(24) Bar-Peled, L.; Kemper, E. K.; Suciu, R. M.; Vinogradova, E. V.; Backus, K. M.; Horning, B. D.; Paul, T. A.; Ichu, T. A.; Svensson, R. U.; Olucha, J.; Chang, M. W.; Kok, B. P.; Zhu, Z.; Ihle, N. T.; Dix, M. M.; Jiang, P.; Hayward, M. M.; Saez, E.; Shaw, R. J.; Cravatt, B. F. Chemical proteomics identifies druggable vulnerabilities in a genetically defined cancer. *Cell* **2017**, *171* (3), 696−709 e23 .
(25) Lanning, B. R.; Whitby, L. R.; Dix, M. M.; Douhan, J.; Gilbert, A. M.; Hett, E. C.; Johnson, T. O.; Joslyn, C.; Kath, J. C.; Niessen, S.; Roberts, L. R.; Schnute, M. E.; Wang, C.; Hulce, J. J.; Wei, B.; Whiteley, L. O.; Hayward, M. M.; Cravatt, B. F. A road map to evaluate the proteome-wide selectivity of covalent kinase inhibitors. *Nat. Chem. Biol.* **2014**, *10* (9), 760−767.
(26) Mertsch, S.; Becker, M.; Lichota, A.; Paulus, W.; Senner, V. Vesicle amine transport protein-1 (VAT-1) is upregulated in glioblastomas and promotes migration. *Neuropathol. Appl. Neurobiol.* **2009**, *35* (4), 342−352.
(27) Mori, F.; Tanigawa, K.; Endo, K.; Minamiguchi, K.; Abe, M.; Yamada, S.; Miyoshi, K. VAT-1 is a novel pathogenic factor of progressive benign prostatic hyperplasia. *Prostate* **2011**, *71* (14), 1579−1586.
(28) Fux, A.; Korotkov, V. S.; Schneider, M.; Antes, I.; Sieber, S. A. Chemical cross-linking enables drafting ClpXP proximity maps and taking snapshots of in situ interaction networks. *Cell Chem. Biol.* **2019**, *26* (1), 48−59 e7 .
(29) Shannon, P.; Markiel, A.; Ozier, O.; Baliga, N. S.; Wang, J. T.; Ramage, D.; Amin, N.; Schwikowski, B.; Ideker, T. Cytoscape: a software environment for integrated models of biomolecular interaction networks. *Genome Res.* **2003**, *13* (11), 2498−2504.
(30) Maere, S.; Heymans, K.; Kuiper, M. BiNGO: a Cytoscape plugin to assess overrepresentation of gene ontology categories in biological networks. *Bioinformatics* **2005**, *21* (16), 3448−3449.
(31) Linial, M.; Levius, O. The protein VAT-1 from Torpedo electric organ exhibits an ATPase activity. *Neurosci. Lett.* **1993**, *152* (1−2), 155−157.
(32) Koch, J.; Foekens, J.; Timmermans, M.; Fink, W.; Wirzbach, A.; Kramer, M. D.; Schaefer, B. M. Human VAT-1: a calcium-regulated activation marker of human epithelial cells. *Arch. Dermatol. Res.* **2003**, *295* (5), 203−210.
(33) Linial, M.; Levius, O. VAT-1 from Torpedo is a membranous homologue of zeta Crystallin. *FEBS Lett.* **1993**, *315* (1), 91−94.
(34) Klapholz, B.; Brown, N. H. Talin - the master of integrin adhesions. *J. Cell Sci.* **2017**, *130* (15), 2435−2446.

DOI: 10.1021/acscentsci.9b00266
ACS Cent. Sci. 2019, 5, 1170−1178